Structure and Photophysics of Deazabipyridyls. Excited Internally Hydrogen-bonded Systems with One Proton Transfer Reaction Site

Łukasz Kaczmarek,[a] Roman Balicki,[a] Janusz Lipkowski,[b] Paweł Borowicz[b] and Anna Grabowska[b]
[a] *Institute of Organic Chemistry, Polish Academy of Sciences, Kasprzaka 44, 01-224 Warsaw, Poland*
[b] *Institute of Physical Chemistry, Polish Academy of Sciences, Kasprzaka 44, 01-224 Warsaw, Poland*

Two deazabipyridyls, 2-(2-hydroxyphenyl)pyridin-3-ol **1** and 2-(2-pyridyl)phenol **2**, are the objects of X-ray and spectroscopic studies. Their syntheses, crystal structures and photophysics in comparison with [2,2'-bipyridyl]-3,3'-diol and [2,2'-bipyridyl]-3-ol **3** are described. The influence of the molecular structure on the efficiency of the proton-transfer reaction in the S_1 state is discussed. The experimental data are compared with semiempirical quantum chemical calculations.

Internally hydrogen-bonded molecules, derivatives of bipyridyl, have been the objects of extensive studies and are reported as very peculiar systems from an academic, as well as practical point of view.[1,2] The most important conclusions of several papers published recently, are as follows: symmetric, planar molecules with two equivalent internal hydrogen bonds, like the parent system, [2,2'-bipyridyl]-3,3'-diol [$BP(OH)_2$], undergo an efficient excited state intramolecular double proton transfer (hereafter ESIPT) accompanied by a very strong, largely Stokes shifted fluorescence. This mechanism was proved

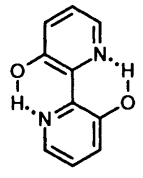

$BP(OH)_2$

by the application of electrooptical absorption and emission measurements (EOAM and EOEM) leading to the determination of the dipole moment of the excited state phototautomer[3] and its Franck–Condon excited precursor.[4] $BP(OH)_2$ is also known as the efficient photostabilizer of polymers,[5,6] fluorescence standard[7] and the lasing dye.[8]

In the present paper we show a selection of structures representing the reduction of symmetry of $BP(OH)_2$ by elimination of one PT reactivity centre. The second internal hydrogen bond, however, is left untouched, rendering the single PT process upon excitation still possible.

The present study compares three molecules shown in Fig. 1, namely 2-(2-hydroxyphenyl)pyridin-3-ol **1**, 2-(2-pyridyl)phenol **2** and [2,2'-bipyridyl]-3-ol **3** abbreviated as HPP, PP and BPOH, respectively.

The demand for new model compounds became, in this case, a challenge for organic synthesis that will be described below together with X-ray analysis. Both preceed the photophysical experiments reported in the last section of the paper.

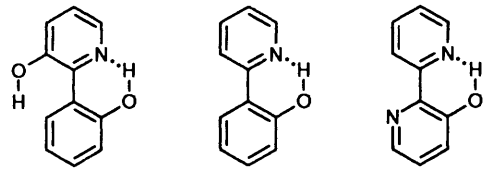

1 **2** **3**

Fig. 1 Formulae of investigated molecules

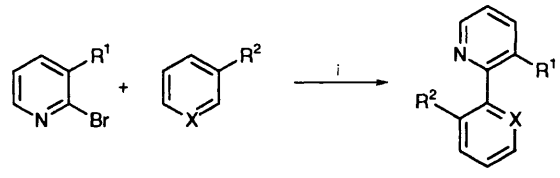

Fig. 2 Scheme of synthesis

Experimental

Room temperature absorption spectra were measured on a Shimadzu UV 3100 spectrophotometer controlled by an IBM PC computer. The corrected fluorescence emission, its excitation spectra and low temperature absorption were measured on a Jasny[9] spectrofluorimeter provided with a photon counting system and an IBM PC computer.

Melting points were observed on a Kofler-type apparatus and are uncorrected. Mass spectra (−70 eV) were obtained on an Intectra AMD-604 spectrometer. IR spectra were measured in KBr (unless otherwise stated) on a Beckman 4240 spectrophotometer. ^1H NMR spectra were recorded at 200 MHz on a Varian Gemini 200 spectrometer in $CDCl_3$ with Me_4Si (TMS) as internal standard, and the chemical shifts are expressed in ppm (coupling constant J in Hz). Column chromatography was carried out using Merck Kieselgel 60 (230–400 mesh). The purity of compounds was checked out by TLC using Merck DC-Alufolien Kieselgel F_{254}.

Solvents for synthesis. All solvents were distilled prior to use. Diethyl ether, tetrahydrofuran (THF) and toluene were dried using standard procedures. Compound **4**[10] and $Pd(PPh_3)_4$[11] were prepared according to the literature methods.

Solvents for photophysical experiments. 3-Methylpentane (3MP) was purified chromatographically on Al_2O_3 and silica gel; butanol 'for fluorescence spectroscopy' (BuOH), Merck, was additionally distilled before use to remove traces of water. All solutions were prepared in a dry box, care was taken to avoid contact with the open air.

Synthesis.—The synthesis of three nonsymmetric biaryls shown in Fig. 1 was performed with the application of the Grignard type reaction leading to biaryls composed of two structurally different aromatic rings.[12] This synthesis is already briefly reported in our review article.[13]

Although compounds **1–3** are already known[14,15,17–19] their syntheses are rather difficult and ineffective. The first general and facile preparation of these compounds is reported herein.

2-(2-*Hydroxyphenyl*)*pyridin*-3-*ol* (*HPP*) **1**.[15] A solution of 2-methoxyphenylmagnesium bromide **6** [obtained from 2-bromoanisole (3.7 g, 20 mmol) and magnesium (1.2 g) in diethyl

ether (50 cm^3)] was added dropwise to a stirred solution of 2-bromo-3-methoxypyridine **4** (3.8 g, 20 mmol) and $Pd(PPh_3)_4$ (1.2 g, 5 mol%) in toluene (50 cm^3), under argon atmosphere, at 50–70 °C. The whole was heated for 1 h, until the temperature reached 100 °C, cooled, diluted with water (100 cm^3) and extracted with chloroform (6 × 50 cm^3). The extract was then washed with 10% HCl (3 × 100 cm^3) and water (1 × 100 cm^3). The combined aqueous layers were neutralized with ammonia, extracted with chloroform (6 × 50 cm^3) and the extract was dried ($MgSO_4$) and evaporated. The residue was purified on a short silica column [eluent hexane–acetone (10:1)] to give 3-methoxy-2-(2-methoxyphenyl)pyridine **8** (yield 2.7 g, 66%), creamy crystals, mp 107–108 °C (from hexane), *m/z* 215 ($M^{\bullet+}$, 19%); ν_{max}/cm^{-1} 1465, 1425, 1280, 1240 and 760; δ_H 8.30 (t, 1 H, *J* 3), 7.39–7.32 (m, 2 H), 7.26 (d, 2 H, *J* 3), 7.06 (dd, 1 H, *J* 7, 1), 6.99 (dd, 1 H, *J* 7, 1), 3.80 (s, 3 H) and 3.78 (s, 3 H) (Found: C, 72.4; H, 6.0; N, 6.5. $C_{13}H_{13}NO_2$ requires C, 72.5; H, 6.1; N, 6.5%).

Compound **8** (2.2 g, 10 mmol) was added to 36% HCl (20 cm^3) and the solution was heated in a sealed tube at 125–130 °C for 12 h. After cooling the reaction mixture was diluted with water (100 cm^3), neutralized with $NaHCO_3$ and extracted with chloroform (6 × 30 cm^3). The extract was dried ($MgSO_4$), the solvent evaporated and the residue purified on a short silica gel column [eluent hexane–acetone (5:1)] to afford product **1** (yield 1.3 g, 70%), yellow crystals, mp 93–99 °C (from chloroform–hexane), *m/z* 187 ($M^{\bullet+}$, 55%); ν_{max}/cm^{-1} 3100–2510, 1530, 1450, 1430, 1320, 1290 and 750; δ_H 8.15 (dd, 1 H, *J* 5, 1.5), 8.14 (dd, 1 H, *J* 8, 1.5), 7.36 (dd, 1 H, *J* 8, 1.5), 7.31 (ddd, 1 H, *J* 8, 7, 1.5), 7.19 (dd, 1 H, *J* 8, 5), 7.07 (dd, 1 H, *J* 8, 1.5) and 6.94 (ddd, 1 H, *J* 8, 1.5) (Found: C, 66.9; H, 5.3; N, 6.9. $C_{11}H_9NO_2 + \frac{1}{2}H_2O$ requires C, 67.3; H, 5.1; N, 7.1%).

2-(2-*Pyridyl*)*phenol* (*PP*) **2**. The reaction of **6** (20 mmol) and 2-bromopyridine **5** (3.2 g, 20 mmol) and work-up of the reaction mixture were carried out as above to give 2-(2-methoxyphenyl)-pyridine **9** (yield 3.3 g, 89%), colourless oil (picrate, mp 155–156 °C[16]), *m/z* 185 ($M^{\bullet+}$, 97%); ν_{max}/cm^{-1}(film) 1600, 1585, 1495, 1460, 1420, 1255, 1240, 1020 and 745; δ_H 8.70 (ddd, 1 H, *J* 5, 2, 1), 7.83–7.74 (m, 2 H), 7.69 (td, 1 H, *J* 8, 2), 7.38 (ddd, 1 H, *J* 8.5, 7.5, 2), 7.20 (ddd, 1 H, *J* 8, 5, 1.5), 7.08 (td, 1 H, *J* 7.5, 1), 7.00 (dd, 1 H, *J* 8.5, 1) and 3.85 (s, 3 H) (Found: C, 77.3; H, 6.0; N, 7.7. $C_{12}H_{11}NO$ requires C, 77.8; H, 6.0; N, 7.6%).

Compound **9** (1.85 g, 10 mmol) was converted into phenol **2** (yield 1.4 g, 82%) by heating in 36% HCl as above and the product was purified on a short silica gel column [eluent hexane–acetone (10:1)], colourless crystals, mp 51–52 °C (from hexane) (oil, bp 135–145 °C/2 Torr[17]), *m/z* 171 ($M^{\bullet+}$, 100%); ν_{max}/cm^{-1} 3050–2300, 1590, 1500, 1470, 1430, 1240 and 750–740; δ_H 8.52 (ddd, 1 H, *J* 5, 2, 1), 7.86 (dt, 1 H, *J* 8, 1), 7.83 (dd, 1 H, *J* 7, 1.5), 7.80 (dd, 1 H, *J* 8, 2), 7.32 (ddd, 1 H, *J* 8, 7, 1.5), 7.25 (ddd, 1 H, *J* 8, 5, 1.5), 7.03 (dd, 1 H, *J* 8.5, 1.5) and 6.92 (ddd, 1 H, *J* 8, 7, 1.5) (Found: C, 77.1; H, 5.3; N, 8.2. $C_{11}H_9NO$ requires C, 77.2; H, 5.3; N, 8.2%).

[2,2′-*Bipyridyl*]-3-*ol* (*BPOH*) **3**. The reaction of 2-pyridylmagnesium bromide **7** [obtained from 2-bromopyridine **3** (3.2 g, 20 mmol) and magnesium (1.2 g) in THF (50 cm^3)] with 2-bromo-3-methoxypyridine **4** (3.8 g, 20 mmol) and work-up of the reaction mixture were carried out as for compound **8**. The product was purified on a short silica gel column [eluent hexane–acetone (3:1)] to give 3-methoxy-2,2′-bipyridyl **10** (yield 1.5 g, 40%), yellow oil (colourless oil[18]), *m/z* 186 ($M^{\bullet+}$, 73%); ν_{max}/cm^{-1}(film) 1580, 1460, 1430–1420, 1270, 800 and 745; δ_H 8.78 (ddd, 1 H, *J* 5, 2, 1), 8.38 (dd, 1 H, *J* 4, 2), 7.86 (ddd, 1 H, *J* 8, 1.5, 0.5), 7.77 (td, 1 H, *J* 7, 2), 7.34–7.26 (m, 3 H) and 3.87 (s, 3 H).

Compound **10** (0.9 g, 5 mmol) was converted into bipyridinol **3** (yield 0.6 g, 70%) by heating in 36% HCl as above and the product was purified on the short silica gel column [eluent hexane–acetone (5:1)], yellow crystals, mp 91–92 °C (from hexane) (mp 92 °C,[18] 88–90 °C[19]), *m/z* 172 ($M^{\bullet+}$, 100%); ν_{max}/cm^{-1} 2900–2400, 1600, 1590, 1500, 1475, 1455, 1440, 1280, 800 and 740; δ_H 8.60 (dt, 1 H, *J* 8, 1), 8.51 (dq, 1 H, *J* 5, 1), 8.21 (dd, *J* 4.5, 1.5), 7.92 (td, 1 H, *J* 8, 1.5), 7.38–7.31 (m, 3 H), 7.24 (dd, 1 H, *J* 8, 4.5) (Found: C, 69.9; H, 4.5; N, 16.1. $C_{10}H_8N_2O$ requires C, 69.8; H, 4.7; N, 16.3%).

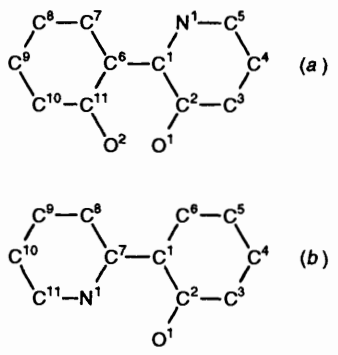

Atom numbering in HPP (*a*) and PP (*b*)

The Crystal Structure Analysis.—X-Ray intensity data were collected on a computer-controlled CAD4 (Enraf–Nonius) diffractometer. The structures were solved by direct methods using SHELX86,[20] and refined by the SHELX76 program (see Table 1).*[21,22]

Results

Two compounds **1** (HPP) and **2** (PP) were subjects of X-ray analysis, and the results were compared with two related molecules, BPOH and $BP(OH)_2$ reported already.[23]

Crystal Structure Analysis.—Crystal structure of HPP. The HPP molecule is a particularly interesting object for X-ray analysis. The possibility of formation of the intra- as well as inter-molecular hydrogen bonds makes its crystal structure not easily predictable.

There are four molecules of HPP **1** of different geometry in the asymmetric unit, as depicted in Figs. 3 and 4(*d*).

Molecular structure. The molecules A and B have similar, though non-identical geometry. The twist angles between the planes defined by, respectively, pyridyl and phenyl rings are 39.3(2) in A and 36.6(2) in B; the difference being much above the limits of error. It may, perhaps, be ascribed to different patterns of inter- and intra-molecular hydrogen bonding of the two molecules, as discussed further on.

The third molecule, denoted C, shows another type of conformation in which an O–H • • • N intramolecular hydrogen bond is formed rather than O–H • • • O as in A and B. The C molecule is flattened as compared with the former two; the twist angle of the two aromatic rings being equal 32.8(2).

The fourth molecule (D) is located in the structure in such a way that its geometrical centre is close to the centre of symmetry (at $\frac{1}{2}$,0,0); the molecule being thus disordered over two orientations, as illustrated in Fig. 4. The geometry and location of the molecule was determined in a stepwise procedure as follows. First, the individual maxima which were revealed in the difference Fourier map (after refinement of molecules A, B and C only) were refined as individual C atoms. The result is depicted in Fig. 4(*a*). In addition to rather unreasonable thermal ellipsoids the resulting 'molecule' shows geometric features

* Atomic coordinates, bond lengths and angles, and thermal parameters have been deposited with the Cambridge Crystallographic Data Centre. See Instructions to Authors (1994).

Table 1 Data collection and structure analysis parameters of HPP and PP

	HPP	PP
Molecular formula	$C_{11}H_9NO_2 \cdot 4/7H_2O$	$C_{11}H_9NO$
Crystal size	0.15 mm × 0.20 mm × 0.6 mm	0.2 mm × 0.25 mm × 0.35 mm
Space group	$P\bar{1}$	$Pca2_1$
Unit cell	a = 7.423(1) Å	13.375(4) Å
	b = 13.713(2) Å	5.903(1) Å
	c = 16.795(3) Å	11.0410(3) Å
	α = 93.09(1)°	
	β = 102.16(2)°	
	γ = 95.30(2)°	
	V = 1659.4(5) Å^3	871.7(4) Å^3
	Z = 7	4
Density calculated	1.3113 g cm^{-3}	1.305 g cm^{-3}
Absorption coefficient	7.102 cm^{-1}	6.381 cm^{-1}
	Radiation: graphite monochromatized Cu-Kα	
Number of reflections:		
measured	7539	1108
unique	6982	970
used in structure analysis	2634	878
Final R values		
unweighted	0.072	
$w = 4.88/\delta(F \times F)$	0.067	0.051
Residual extreme in final difference map/e Å^{-3}		
	+0.44	+0.17
	−0.47	−0.16

which may be considered unlikely. These are a coplanar arrangement of the pyridyl and phenyl rings of the molecule and the C(1D)–C(6D) bond distance which was found to be 1.36 Å. Then, the next step of structure refinement was done by using rigid moieties of hydroxyphenyl and hydroxypyridyl rings of geometry arbitrarily taken as that of molecule A. The two moieties were located with half occupancy at positions corresponding to best geometrical fit to the molecule shown in Fig. 4(*a*). The final refinement was then performed with the two moieties treated as independent rigid bodies, with half occupancy each and with isotropic thermal parameters fixed to just one free variable. The result is depicted in Fig. 4(*b*) through to 4(*d*). As may be seen the molecule shows a rather 'normal' bond length C(1)–C(6) = 1.523(7) Å, also a twisted conformation [the interplanar angle = 8.7(2)°] seems a more realistic situation than coplanarity.

Hydrogen bonding and crystal packing. In the following text, the symbols a, b, c, d, 1w and 2w refer to A, B, C, D modifications of HPP, and two water molecules shown in Fig. 5, respectively.

The conformational difference between molecules A and B is accompanied by a difference in the intramolecular hydrogen bond: the O(1a)···O(2a) distance (2.53 Å) is longer than that between O(1b) and O(2b) (2.44 Å). There is also a difference between A and B in internal geometry: the C(6a)–C(11a)–O(2a) bond angle is greater than C(6b)–C(11b)–O(2b) by 2.9(7)°. The intramolecular distance between hydrogen bonded atoms in molecule C [O(2c) and N(1c)] is 2.63 Å. Geometry of the molecule around the N atom differs from that in molecules A and B, in particular, the C–N–C angle is smaller here than that in A by 2.8(8)° and in B by 3.8(8)°.

Despite the fact that the crystals were grown from a non-aqueous solution there are two water molecules present per 3.5 molecules of HPP.

Water plays here an important role in determining the pattern of intermolecular interactions, as illustrated in Fig. 5. The O(1w) is hydrogen bonded to O(1w)′ [O(1w)′ stands for the water molecule, 1w, inverted by centre of symmetry at $\frac{1}{2}$, $\frac{1}{2}$, $\frac{1}{2}$], and to O(1a) and N(1b); thus bridging molecules A and B. The O(1w)···O(1a) and O(1w)′···N(1b) distances (2.78 and 2.77 Å, respectively) correspond to rather typical hydrogen bonds. On the other hand, the O(2w) is hydrogen bonded to O(2b) (2.84 Å) and N(1a) (2.80 Å) thus contributing to the intermolecular bonding pattern between A and B. Similarly to O(1w) the O(2w) molecules are arranged pairwise by symmetry centres [at $\frac{1}{2},\frac{1}{2},0$ for O(2w)]. The molecule C is hydrogen bonded to A *via* an O(1c)···O(1a) short contact (2.60 Å). The molecule D, in each of its two orientations around the centre of symmetry is hydrogen bonded to a B molecule [O(2d)···O(1b) distance is 2.65 Å].

Crystal structure of PP. In contrast to the rather complicated crystal structure of HPP, the PP **2** molecule existing in one planar conformer builds a very simple crystal composed of monomers internally linked by one hydrogen bond each. No symptoms of intermolecular interactions are noted.

The results of X-ray analysis are reported quite similarly as above, in Table 1 and Figs. 6 and 7.

Selected data on the molecular structure of PP are as follows: both rings are coplanar, the interatomic distances: C–O, N···O, O–H, H···N are 1.353, 2.54, 1.02 and 1.67 Å, respectively and the O–H–N angle, 140°. All this makes the PP molecule very similar to the earlier reported BPOH structure. This analogy and the photophysical consequences will be discussed subsequently.

Photophysics of PP and HPP as compared with BPOH.—All three molecules may be regarded as the modification of the symmetric parent structure of $BP(OH)_2$ that was already reported as a system undergoing double PT upon excitation. It was also shown previously that a weak perturbation of the molecular framework by methyl substitution on one aromatic ring, in position 4, does not change the basic photophysical properties of $BP(OH)_2$.[3,4,6] The next step would be the investigation of the model systems representing the strong perturbation of symmetry of $BP(OH)_2$ by the elimination of one internal hydrogen bond. Thus, absorption and fluorescence, their excitation spectra and fluorescence quantum yields of HPP and PP will be compared with BPOH, also previously

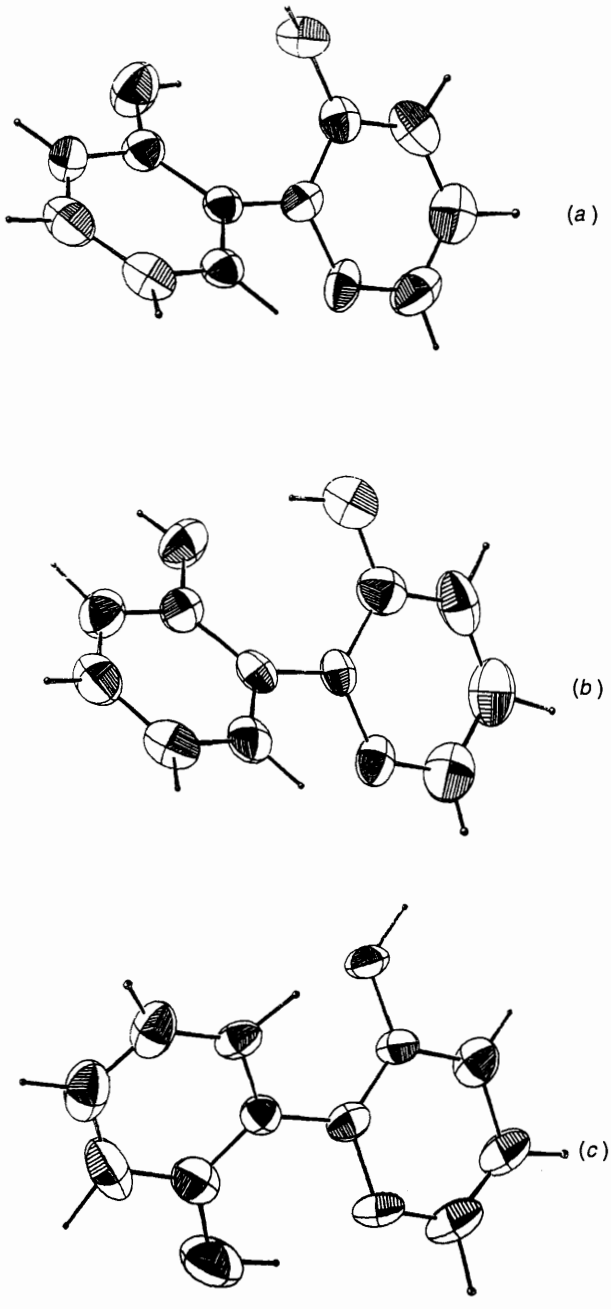

Fig. 3 ORTEP[22] plot of the three symmetrically independent molecules A, B, C of HPP which do not show orientational disorder. Ellipsoids are drawn at 50% probability level; hydrogen atoms are given arbitrary 0.1 Å radii.

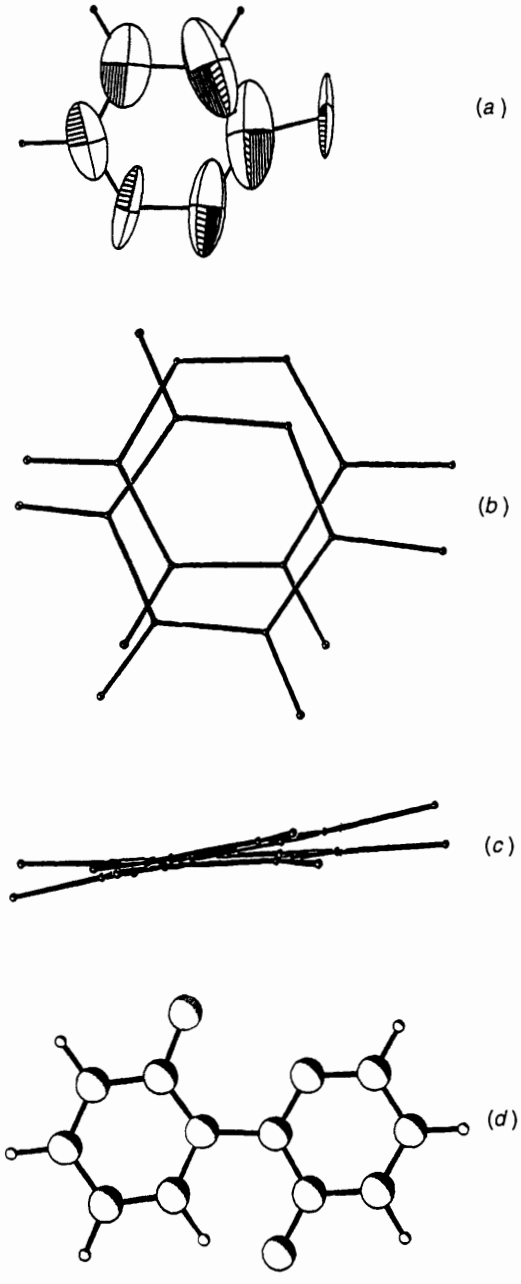

Fig. 4 Illustration of disordering of the molecule D: (*a*) ORTEP plot of the results of anisotropic refinement of individual atoms; (*b*) superposition of hydroxyphenyl and hydroxypyridyl moieties refined (with half occupancy each) as rigid bodies, projected onto the molecular plane and, (*c*) as (*b*) but viewed perpendicularly; (*d*) plot of the fourth (D) symmetrically independent molecule of HPP (all atoms are given arbitrary 0.1 Å radii)

studied and reported.[24] Quantum chemical calculations will be compared with experimental data where possible. The main feature of the model structures is their more pronounced flexibility as compared with the parent molecule which is strongly kept in planar geometry by the two internal hydrogen bonds.

Absorption, fluorescence and its excitation spectra. In Fig. 8 there are shown absorption spectra of both molecules, HPP and PP and the excitation energies of most important transitions calculated with the INDO/S method. For HPP two rotamers are included into the picture: the 'open' rotamer and the 'closed' one.

The result of a search of the phototautomerism of HPP in a non-interacting solvent is shown in Fig. 9. Indeed, the characteristic strongly Stokes shifted fluorescence was found. The extent of the Stokes loss (*ca.* 10 000 cm^{-1}) and the wavenumber of fluorescence maximum (*ca.* 19 000 cm^{-1}), leave little doubt on the origin of this emission being in close analogy to the fluorescence of $BP(OH)_2$. Two important differences are however to be noticed: at room temp. the fluorescence of HPP was extremely weak, and its excitation spectrum was shifted considerably to the red in respect to absorption band. No fluorescence from the primary excited enol tautomer was detected at any temperature.

In the next experiment (Fig. 10) butanol was used in order to show how much the photophysics of HPP is changed in a protic solvent. Here, at room temp. the phototautomeric fluorescence was strong enough to be easily detected and the excitation spectrum could be measured with very good accuracy. The striking feature was again observed: the phototautomerisation process selects only some structures from the total ensemble of absorbing species, namely those of lowest energy.

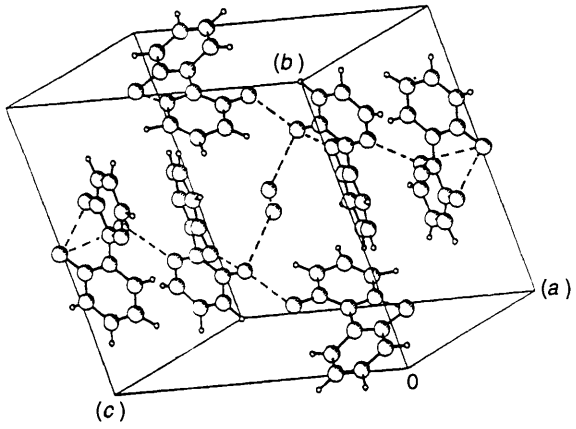

Fig. 5 Molecular packing in the crystal structure of HPP and hydrogen bonding pattern (dotted lines)

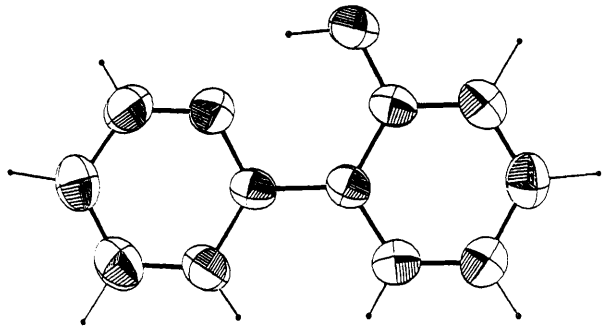

Fig. 6 ORTEP[22] plot of PP. Ellipsoids are drawn at 50% probability level; hydrogen atoms are given arbitrary 0.1 Å radii.

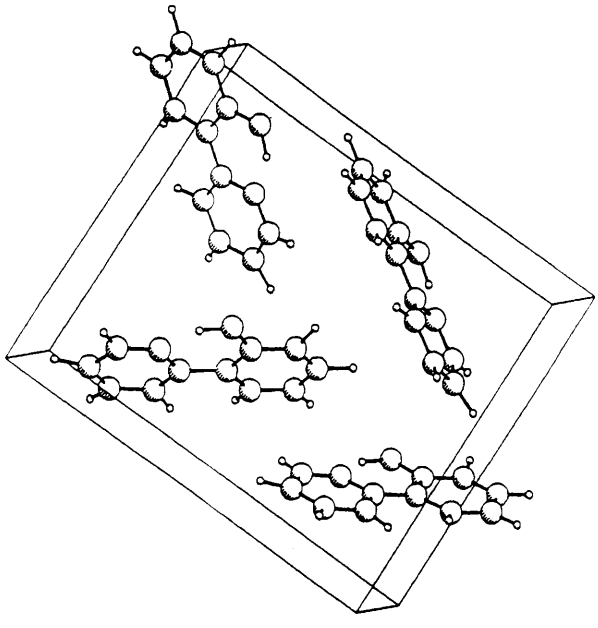

Fig. 7 Molecular packing in the crystal structure of PP

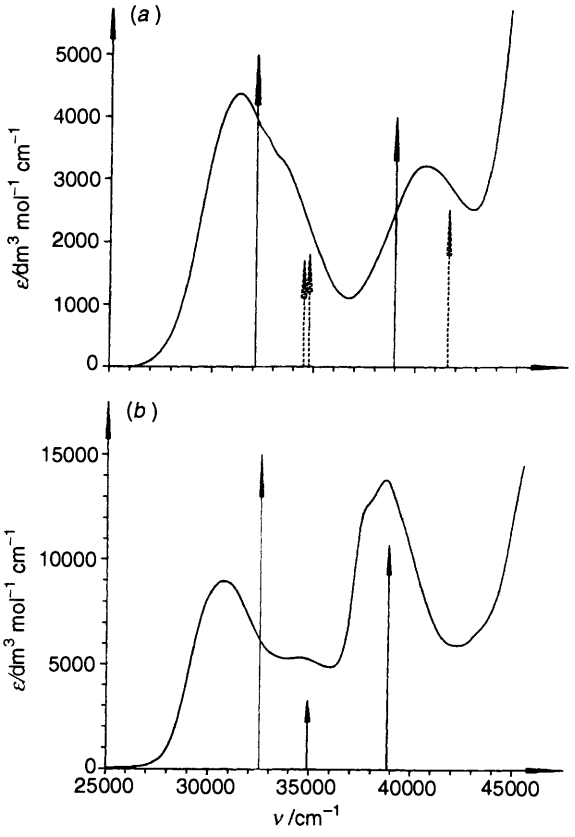

Fig. 8 Room temp. absorption spectra of HPP (*a*) and PP (*b*); solvent 3MP. Arrows denote the INDO/S calculated transition energies for optimized structures. Dashed arrows – transitions calculated for the open conformer of HPP. The length of each arrow is proportional to the calculated oscillator strength.

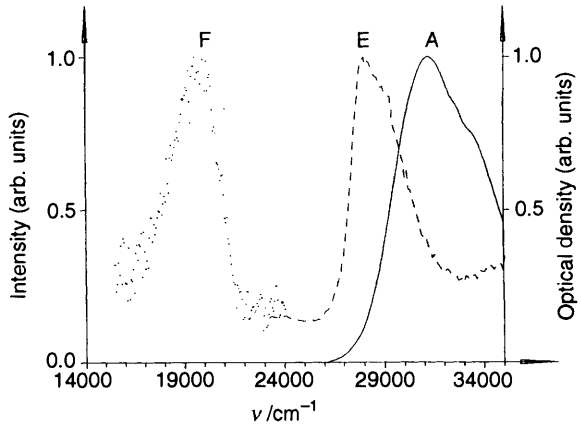

Fig. 9 Absorption (A), fluorescence (F), excited at $\nu \simeq 27\,800$ cm^{-1}, and fluorescence excitation (E), observed at $\nu \simeq 20\,000$ cm^{-1}, spectra of HPP measured in 3MP at room temp.

The model compound, shown in Fig. 10, is very helpful here and will be discussed below. The complicated photophysical behaviour of HPP can be anticipated in view of the structural complexity shown by the X-ray analysis.

From this point of view the PP molecule is much simpler, and such is its photophysics, shown in Fig. 11. This is an extremely weakly fluorescent species. Only low temperature emission could be detected. The corresponding fluorescence excitation spectrum could not be determined, because of the very high concentration of the compound needed to observe the emission.

Quantum Chemical Calculations.—HPP and PP molecules were calculated along with BP(OH) for comparison. The geometry of molecules was optimized with the MOPAC 5.0-PM3 method[25] successfully used earlier for geometry optimization of bipyridyldiols.[4] The transition energies for optimized geometries were calculated with the INDO/S method using the original Ridley and Zerner parametrization.[26] To find all possible rotamers of the form stable in the ground state the total energy of each molecule *vs.* the dihedral angle between the rings was calculated by MOPAC. The angle increment used was 5°, the distances and angles were optimized for each position of the rings.

The calculation results of the total energy as a function of the dihedral angle between the rings are the following: (*i*) for BPOH and PP one minimum was obtained (planar molecules); (*ii*) for HPP two rotamers are possible:—the first one with the dihedral

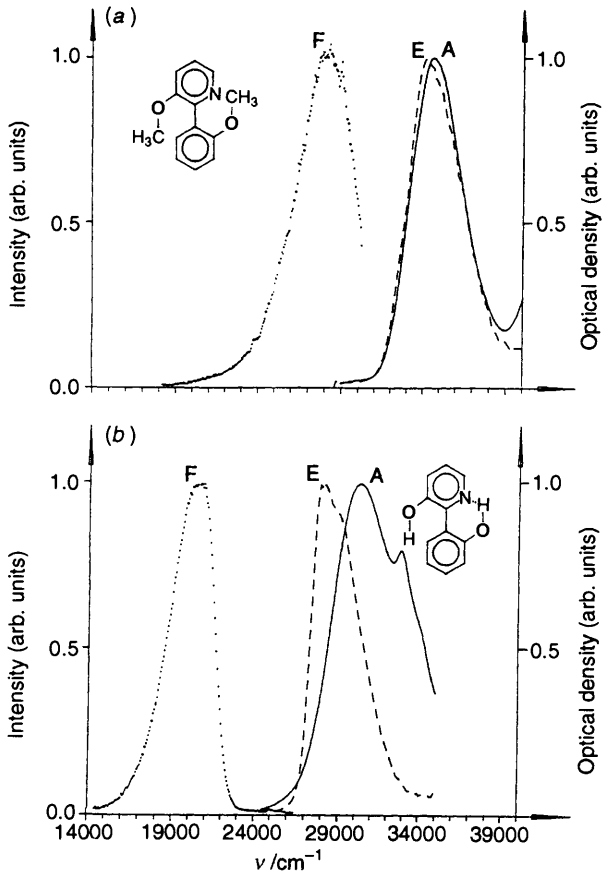

Fig. 10 Absorption (A), fluorescence (F) and its excitation (E) spectra in BuOH at room temp.; HPP (*b*) and its dimethoxy derivative (*a*), $\tilde{\nu}_{excit}$ equals 27 800 cm^{-1} and 33 000 cm^{-1} for HPP and model compound, respectively, $\tilde{\nu}_{obs}$ = 19 500 cm^{-1} and 27 000 cm^{-1} for HPP and model compound, respectively

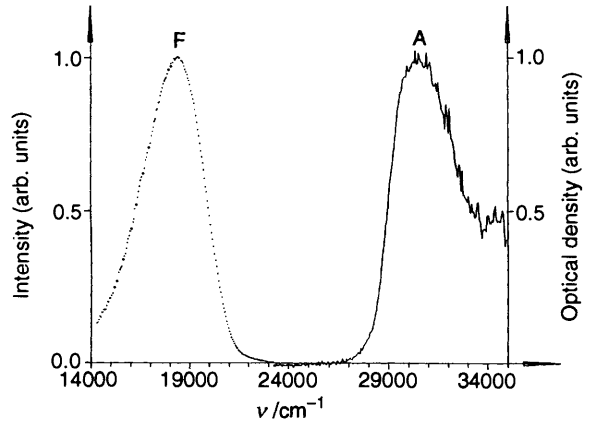

Fig. 11 Absorption (A) and fluorescence (F) spectra of PP measured in 3MP at 77 K, concentration *ca.* 10^{-3} mol dm^{-3}

angle of about 70°, called hereafter the 'open structure',—the other one, distorted by about 30°, the 'closed structure'. The second (closed) rotamer of HPP can provide the PT reaction in the S_1 state. The results of calculations are shown in Fig. 12.

Two rotamers of HPP are separated by the potential barrier. One minimum around the angle of twist about 30° is well shaped, while the other, a shallow one, corresponds to several, almost isoenergetic conformations, close to the perpendicular geometry of the two aromatic rings. Both rotamers are nicely recognized by the experiment and will be discussed below.

The geometry optimisation gives the results that remarkably agree with the experimental crystal structure data. The most

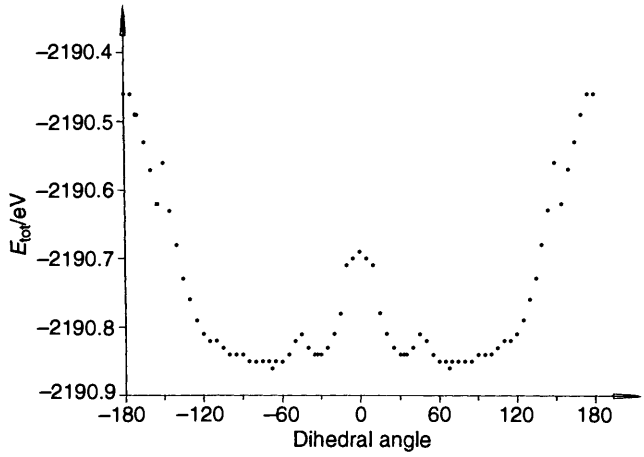

Fig. 12 Total energy of enol tautomer of HPP molecule as calculated with MOPAC 5.0-PM3 as a function of dihedral angle, see text

Table 2 Comparison of selected X-ray and MOPAC data[a]

	X-Ray	MOPAC-PM3
HPP		
O(1)–C(2)	1.353(7)	1.364
N(1)–C(1)	1.371(8)	1.370
O(2)–C(11)	1.382(8)	1.360
C(1)–C(6)	1.477(7)	1.473
C(1)–N(1)–C(5)	119.0(5)	121.3
C(2)–C(1)–C(6)	124.8(5)	126.1
O(1)–C(2)–C(3)	121.6(5)	114.2
O(2)–C(11)–C(10)	115.5(6)	115.4
PP		
O(1)–C(2)	1.353(4)	1.355
C(1)–C(6)	1.382(5)	1.382
N(1)–C(7)	1.356(5)	1.369
C(1)–C(7)	1.481(5)	1.467
C(7)–N(1)–C(11)	119.9(3)	120.2
O(1)–C(2)–C(3)	117.0(3)	115.0
C(1)–C(7)–C(8)	122.8(3)	122.2

[a] Distances/Å; angles (°).

representative examples of bond distances and angles are compared in Table 2.

After a geometry optimization procedure the transition energies of $^1(\pi,\pi^*)$ and $^1(n,\pi^*)$ states for all primary structures and phototautomers of each molecule were calculated by the INDO/S method. The results are shown in Fig. 13.

The existence of the 'driving force' for the ESIPT reaction understood as a change of electron density upon electronic excitation of a molecule, similar to that calculated previously for $BP(OH)_2$ and BPOH [1,24] was confirmed also for PP and HPP.

Discussion

Several points will be discussed: (*i*) the structural limitations of the efficient phototautomerization in the molecular framework of bipyridyl linked by intramolecular hydrogen bond/s; (*ii*) the results of X-ray analyses as related to photophysical properties of compounds under study; (*iii*) non-symmetric biaryls as a challenge for modern organic synthesis.

The idea to study the photophysics of the molecules being the subject of the present work emerged from our previous experiments summed up in the introduction. 'The defected bipyridyldiols' as we call them, turned out to be extremely interesting objects from the point of view of the mechanism of ESIPT reactions. First, the requirement of obtaining the non-symmetric biaryls by the efficient, relatively simple synthesis, uncomplicated by the tedious procedure of chemical separation

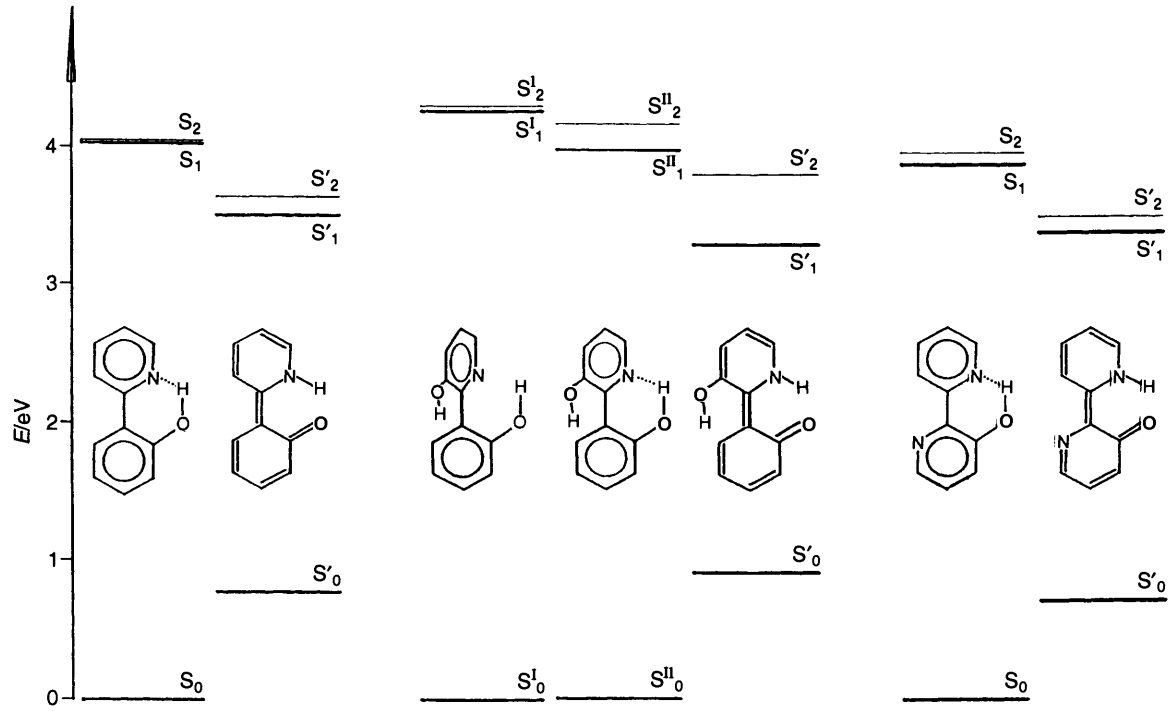

Fig. 13 INDO/S calculation results of the lowest transition energies of enol (primary) and ketotautomers of PP, rotamers I and II of HPP and BPOH; for excited the states: thick lines (π,π^*) levels, thin lines (n,π^*) levels

Table 3 Comparison of calculated with MOPAC and evaluated from spectroscopic data N–O distances in hydrogen-bonded systems

	N–O/Å	
Compound	Calc.	Expl.
$BP(OH)_2$	2.7	2.56
BPOH	2.7	2.57
HPP	2.7[a]	2.63[b]
PP	2.7	2.54

[a] The value calculated for rotamer II of HPP. [b] The value obtained for molecule C (see crystal structure analysis).

of all possible condensation products, led us to the Grignard type of reaction.[1,2] Thus, BPOH, HPP and PP were obtained directly, with quite satisfactory yields. These three molecules represent all possible modifications of the $BP(OH)_2$ structure leading to the exclusion of one internal hydrogen bond. This strong modification of the parent structure results in the large reduction of the intensity of phototautomeric fluorescence.

The examination of the results of the X-ray analysis reported above confirm the earlier observation:[1] the planarity of the internally hydrogen-bonded molecule is not a decisive factor for the efficient phototautomeric fluorescence. Thus BPOH and PP are planar (see X-ray data and ref. 23) like the strongly fluorescent $BP(OH)_2$. The lengths of internal hydrogen bonds do not distinguish them either. The corresponding N–O distances are compared below.

The N–O distances of Table 3 are short and almost identical. The HPP molecule is distinguished by its non-planarity which is reflected in the increase of the N–O distance and several photophysical consequences of that. The study of this molecule brings particularly interesting data for comparison of the X-ray analysis, the spectroscopic results and theoretical calculations.

The crystal structure of HPP reported and described above shows that in the solid state, there is a definite tendency to build the intermolecular, not only intramolecular hydrogen bonds (Fig. 5). Moreover, the HPP molecules 'look for water' in order to stabilize their solid state structure. Another interesting observation is that the crystal structure accepts four modifications of the HPP molecule, differing by several degrees (9–39) of the dihedral angle. Thus the HPP molecule is relatively soft. The distortion from coplanarity is reproduced nicely by the theoretical calculations shown in Fig. 12, where the first minimum corresponds to the twist angle about 30°. From among four different modifications of the HPP structure present in the crystal lattice, only two contain the intramolecular hydrogen bond preparing the system for phototautomerization. Another two may be identified with the open structures predicted by the calculation. Thus, the solid state data may be helpful for understanding the spectral behaviour of HPP shown in Figs. 9 and 10. In both solvents, inert 3MP and protic BuOH, the phototautomeric fluorescence, apart from the intensity, is very similar; the same concerns the excitation spectra (curves E). In both solvents they agree perfectly, while the absorption spectra show clearly the stabilizing effect of the hydrogen-bonding properties of BuOH.

This demonstrates that the tautomerization reaction selects the conformers with the lowest energy absorption—the internally hydrogen-bonded molecules. These are in both solvents obviously identical. The existence of the open structures is confirmed by the absorption spectrum of the model compound, a derivative of HPP with both active protons replaced by methyl groups [Fig. 10(*a*)]. Its absorption maximum is close to the high energy shoulder in the absorption spectrum of HPP [Fig. 10(*b*)]. The fluorescence of the open structures of HPP may also be detected, but at low temperature, which is not shown here.

Moreover, the energy differences between the absorption and fluorescence excitation maxima are *ca.* 3000 and 2000 cm^{-1}, for 3MP and BuOH respectively. This is astonishingly near to the calculated energy differences between the open and closed rotamers shown as full and dotted arrows in Fig. 8.

Finally let us stress the most fundamental differences between a parent structure, a 2,2′-bipyridyl (BP), a doubly hydrogen bonded $BP(OH)_2$ and the defected structures studied in the present work: BPOH, PP and HPP.

First, the introduction of an additional depopulation channel,

Table 4 Quantum yields (η_f) and fluorescence lifetimes (τ_f) of $BP(OH)_2$, BPOH, HPP and PP in: 3-methylpentane (3MP) and butanol (BuOH), at room temp.

Molecule (Solvent)	η_f	τ_f/ns
$BP(OH)_2$[a]		
(3MP	$(3.2 \pm 0.6) \times 10^{-1}$	2.98 ± 0.03
BuOH)	$(3.6 \pm 0.7) \times 10^{-1}$	—
BPOH[a]		
(3MP	$(5.5 \pm 1.1) \times 10^{-3}$	3.02 ± 0.03
BuOH)	$(2.4 \pm 0.5) \times 10^{-2}$	—
HPP		
(3MP	$(9.0 \pm 3.1) \times 10^{-4}$	—[b]
BuOH)	$(1.7 \pm 0.3) \times 10^{-2}$	2.86 ± 0.03
PP		
(3MP	$< 1 \times 10^{-5}$	—
BuOH)	$< 1 \times 10^{-5}$	—

[a] The η_f data in 3MP are in full agreement with the corresponding results of refs. 7 and 24. Fluorescence was excited at 30 000 cm^{-1}. [b] The lifetime of HPP in 3MP was strongly non-exponential, because of the large contribution of intermolecularly H-bonded dimers.

the very fast ESIPT reaction, results in the lack of phosphorescence. In contrast to BP, all systems undergoing phototautomerization reaction are non-phosphorescent, at least from the primary structures. The second general observation made earlier, is that the necessary condition for generation of the strong fluorescence from the ESIPT reaction product in the molecular framework of 2,2′-bipyridyl is the existence of two equivalent internal hydrogen bonds. Molecules, like PP, HPP and BPOH, are very poor emitters, especially in the inert solvent; this is clearly shown in Table 4. In contrast, the lifetimes of phototautomers, about 3 ns, are relatively stable, demonstrating the common regime of depopulation of fluorescent species.

The effect of the decrease of the tautomeric fluorescence quantum yield was discussed in our earlier paper comparing the depopulation mechanism of BPOH *vs.* $BP(OH)_2$.[24] Briefly: two main factors do contribute to the acceleration of the radiationless processes in this family of molecules: (*i*) a strong coupling of the electronic energy with the torsional motion,[27] (*ii*) the proximity effect [28] of (π,π^*) and (n,π^*) states. This last is particularly well illustrated by the diagram of Fig. 13 and the Table 4: there is an exact correspondence between the proximity of the calculated lowest (π,π^*) and (n,π^*) states and the fluorescence quantum yields, η_f. Thus, the almost non-fluorescent molecule, PP, reveals the exact energetic coincidence of both lowest singlet states. Fig. 13 illustrates another interesting observation: the proximity of (π,π^*) and (n,π^*) states is more pronounced in the primary structures than in phototautomers.

The contribution of the proximity effect is usually verified by the detection of the influence of the protic solvent on fluorescence intensity. Hydrogen-bonding that involves n-electrons raises the energy of (n,π^*) states increasing the corresponding energy gap and restoring the purity of electronic states.[28] This treatment is, however, non-applicable to the internally hydrogen-bonded molecules, like *e.g.* PP, since n-electrons are already bonded. Hence, the effect impressively illustrated by the data of Table 4 has probably no general explanation. Thus a strongly fluorescent system, $BP(OH)_2$, does not suffer any influence of butanol, the other extreme case, an almost non-fluorescent PP, either. Here the proximity (π,π^*) and (n,π^*) states clearly cannot be removed by solvation with BuOH. The case of HPP is most complicated by the existence of externally hydrogen-bonded dimers as stated by X-ray analysis, and present probably also in a dry neutral solvent, like 3MP. In butanol the solubility of HPP is much higher, and the contribution of monomeric molecules able to phototautomerize considerably increases. This is most probably the reason for the strong solvent effect on fluorescence quantum yield shown in Table 4. The only example, a BPOH molecule possessing the naked N atom could serve as a model for the illustration of the proximity effect of $(n,\pi^*)/(\pi,\pi^*)$ states.

Other factors that also may contribute to depopulation kinetics of this group of proton transferring molecules, like the deep stabilization of the twisted intramolecular charge transfer (TICT) states will be discussed in a subsequent paper.

Acknowledgements

This work was partly sponsored by KBN grants No. 2P303 111 04 and 2P302 081 04.

References

1 H. Bulska, *Chem. Phys. Lett.*, 1983, **98**, 398.
2 (*a*) M. Eyal, R. Reisfeld, V. Chernyak, Ł. Kaczmarek and A. Grabowska, *Chem. Phys. Lett.*, 1991, **176**, 531; (*b*) R. Reisfeld and Ch. K. Jorgensen, in *Optical Properties of Colorants or Luminescent Species in Sol–Gel Glasses*, Springer-Verlag, Berlin, Heidelberg, 1991.
3 P. Borowicz, A. Grabowska, R. Wortmann and W. Liptay, *J. Lumin.*, 1992, **52**, 265.
4 R. Wortmann, K. Elich, S. Lebus, W. Liptay, P. Borowicz and A. Grabowska, *J. Phys. Chem.*, 1992, **96**, 9724.
5 A. Grabowska, H. Bulska and G. Rymarz, Pol. Pat. 257 033, 1990.
6 Ł. Kaczmarek, B. Nowak, J. Żukowski, P. Borowicz, J. Sepioł and A. Grabowska, *J. Mol. Struct.*, 1991, **248**, 189.
7 H. Bulska, *J. Lumin.*, 1988, **39**, 293.
8 J. Sepioł, H. Bulska and A. Grabowska, *Chem. Phys. Lett.*, 1987, **40**, 607.
9 J. Jasny, *J. Lumin.*, 1978, **17**, 149.
10 P. Nedenskov, N. Clauson-Kaas, J. Lei, H. Heide, G. Olsen and G. Jansen, *Acta Chem. Scand.*, 1969, **23**, 1791.
11 D. R. Coulson, *Inorg. Synth.*, 1972, **13**, 121.
12 V. N. Kalinin, *Synthesis*, 1992, 413.
13 A. Grabowska and Ł. Kaczmarek, *Pol. J. Chem.*, 1992, **66**, 715.
14 M. L. Martinez, W. C. Cooper and P. Chou, *Chem. Phys. Lett.*, 1992, **193**, 151.
15 Ł. Kaczmarek and P. Nantka-Namirski, *Pol. J. Chem.*, 1992, **66**, 801.
16 T. A. Geissman, M. J. Schlatter, J. D. Webb and J. D. Roberts, *J. Org. Chem.*, 1946, **11**, 741.
17 J. W. Haworth, I. M. Heilbron and D. H. Hey, *J. Chem. Soc.*, 1940, 359.
18 W. Siemanowski and H. Witzel, *Liebigs Ann. Chem.*, 1984, 1731.
19 Ł. Kaczmarek, *Bull. Pol. Acad. Sci. Chem.*, 1985, **33**, 401.
20 G. M. Sheldrick, SHELXS86, in *Crystallographic Computing 3*, ed. G. M. Sheldrick, C. Kruger and R. Goddard, Oxford University Press, 1985, pp. 175–189.
21 G. M. Sheldrick, SHELX76, Program for Crystal Structure Determination, University of Cambridge, 1976.
22 C. K. Johnson, ORTEP, a Fortran Thermal Ellipsoid Plot Program for Crystal Structure Illustrations. Report ORNL-5138 (3rd rev.), Oak Ridge National Laboratory, Oak Ridge, Tenn., 1976.
23 J. Lipkowski, A. Grabowska, J. Waluk, G. Calestani and B. A. Hess, Jr., *J. Cryst. Spectr. Res.*, 1992, **22**, 563.
24 H. Bulska, A. Grabowska and Z. R. Grabowski, *J. Lumin.*, 1986, **35**, 189.
25 (*a*) J. J. P. Stewart, MOPAC 5.0, A General Purpose Molecular Orbital Package (QCEP 455); (*b*) J. J. P. Stewart, *J. Comput. Chem.*, 1989, **10**, 209.
26 J. Ridley and M. Zerner, *Theor. Chim. Acta*, 1973, **32**, 11; 1976, **42**, 223.
27 M. S. Gudipati, *J. Phys. Chem.*, 1993, **97**, 8602 and refs. therein.
28 E. C. Lim, in *Excited states*, ed. E. C. Lim, Academic Press, New York, 1977, vol. 3.

Paper 4/00177J
Received 12*th January* 1994
Accepted 15*th March* 1994